

Proteomic Shift in Mouse Embryonic Fibroblasts Pfa1 during Erastin, ML210, and BSO-Induced Ferroptosis

Olga M. Kudryashova ¹, Alexey M. Nesterenko ², Dmitry A. Korzhenevskii ¹, Valeriy K. Sulyagin ³, Vasilisa M. Tereshchuk ^{1,4}, Vsevolod V. Belousov ^{1,2} and Arina G. Shokhina ^{1,2,4,*}

- ¹ Neurotechnology Laboratory, Federal Center of Brain Research and Neurotechnologies, Federal Medical Biological Agency, 117997 Moscow, Russia; olga.kudryashova179@gmail.com (O.M.K.); litophage@gmail.com (D.A.K.); vasmter@gmail.com (V.M.T.); vsevolod.belousov@gmail.com (V.V.B.)
- ² Shemyakin-Ovchinnikov Institute of Bioorganic Chemistry, Russian Academy of Science, 117997 Moscow, Russia; comconadin@gmail.com
- ³ Faculty of Biology, Lomonosov Moscow State University, 119234 Moscow, Russia; sulyaginvk@gmail.com
- ⁴ Institute of Translational Medicine, Pirogov Russian National Research Medical University, 117997 Moscow, Russia
- * Correspondence: a.g.shokhina@yandex.ru

Abstract: AbstractFerroptosis is a unique variety of non-apoptotic cell death, driven by massive lipid oxidation in an iron-dependent manner. Since ferroptosis was introduced as a concept in 2012, it has demonstrated its essential role in the pathogenesis in neurodegenerative diseases and an important role in therapy-resistant cancer cells. Thus, detailed molecular understanding of both canonical and alternative ferroptosis pathways is required. There is a set of widely used chemical agents to modulate ferroptosis using different pathway targets: erastin blocks cystine–glutamate antiporter, system xc⁻; ML210 directly inactivates GPX4; and L-buthionine sulfoximine (BSO) inhibits γ -glutamylcysteine synthetase, an essential enzyme for glutathione synthesis de novo. Most studies have focused on the lipidomic profiling of model systems undergoing death in a ferroptotic modality. In this study, we developed high-quality shotgun proteome sequencing during ferroptosis induction by three widely used chemical agents (erastin, ML210, and BSO) before and after 24 and 48 h of treatment. Chromatograms were registered in DDA mode and are suitable for further label-free quantification. Both processed and raw files are publicly available and could be a valuable dynamic proteome map for further ferroptosis investigation.

Dataset: Shotgun proteomics are available at the PRoteomics IDentifications (PRIDE) Archive database with the following dataset identifiers: Erastin experiment—PXD041463 (<https://www.ebi.ac.uk/pride/archive/projects/PXD041463>, DOI: 10.6019/PXD041463); ML210 experiment—PXD041327 (<https://www.ebi.ac.uk/pride/archive/projects/PXD041327>, DOI: 10.6019/PXD041327); BSO—PXD041415 (<https://www.ebi.ac.uk/pride/archive/projects/PXD041415>, DOI: 10.6019/PXD041415).

Dataset License: CC-BY-NC

Keywords: ferroptosis; proteomics; LC-MS/MS; mouse embryonic fibroblasts; Pfa1; cell death; glutathione peroxidase 4; erastin; ML210; L-Buthionine-sulfoximine; BSO



Citation: Kudryashova, O.M.; Nesterenko, A.M.; Korzhenevskii, D.A.; Sulyagin, V.K.; Tereshchuk, V.M.; Belousov, V.V.; Shokhina, A.G. Proteomic Shift in Mouse Embryonic Fibroblasts Pfa1 during Erastin, ML210, and BSO-Induced Ferroptosis. *Data* **2023**, *8*, 119. <https://doi.org/10.3390/data8070119>

Academic Editor: Rüdiger Prüss

Received: 13 April 2023

Revised: 30 June 2023

Accepted: 7 July 2023

Published: 12 July 2023



Copyright: © 2023 by the authors. Licensee MDPI, Basel, Switzerland. This article is an open access article distributed under the terms and conditions of the Creative Commons Attribution (CC BY) license (<https://creativecommons.org/licenses/by/4.0/>).

1. Summary

Ferroptosis is a unique type of non-apoptotic regulated cell death whose distinguishing features are its iron-dependent manner and overwhelming lipid peroxidation downstream of metabolic dysfunctions [1]. Lipid peroxidation is stimulated by the presence of iron in the cell, due to its ability to enter into free radical reactions according to the Fenton mechanism and generate reactive oxygen species (ROS) [2]. One of the key regulators of ferroptosis control is glutathione peroxidase 4 (GPX4), which is able to reduce lipid

peroxides, using glutathione (GSH) as an electron donor. This enzyme is a component of the crucial ferroptosis suppressing system—the cyst(e)ine/GSH/GPX4 axis [3]. Currently, a growing number of diseases is associated with redox stress, and many of them have known hallmarks of ferroptosis, such as lipid peroxidation [4].

There are a few widely used drugs for ferroptotic induction, among them, erastin, ML210, and L-buthionine sulfoximine (BSO). All of them inhibit different components of the cyst(e)ine/GSH/GPX4 axis. Erastin can block cystine–glutamate antiporter, system xc⁻, which plays a key role in cystine transportation in cells [5,6]. BSO inhibits γ -glutamylcysteine synthetase, an essential enzyme for de novo glutathione synthesis. Finally, ML210 is the most specific GPX4 inhibitor that directly inactivates it without interacting with other glutathione peroxidases [7].

Using different mechanisms of ferroptosis induction extends the ability of ferroptosis modulation, which could be extremely helpful in understanding the molecular mechanisms of ferroptosis-related diseases and in researching the therapeutic potential of ferroptosis [8–11]. The canonical ferroptosis pathway leads to phospholipid hydroperoxide accumulation; therefore, most studies with omics have focused on lipidomic profiles [12,13].

In this study, we developed a bottom-up shotgun proteomic for three widespread chemical proferroptotic inducers (erastin, ML210, and BSO) at two time points. For each drug, we performed an independent series of liquid chromatography–mass spectrometry (LC-MS/MS) in DDA mode in three conditions: control (without treatment), 24 h, and 48 h after the ferroptosis induction. For each condition, we performed four biological replicates, each in two or three technical replicates. We provided both the raw data and the bioinformatically processed data at the protein level via PRoteomics IDentifications database (PRIDE).

To the best of our knowledge, this is the first comprehensive experimental study that estimates the proteomic shift in mouse embryonic fibroblasts for these three widely used chemical ferroptosis inducers (Erastin, ML210 and BSO). As a valuable dynamic proteome reference, these data could be helpful for further investigation of the role of ferroptosis in disease pathogenesis and searching for new biomarkers in cancer.

2. Data Description

In this study, we presented the proteomic shifts during erastin-, ML210-, and BSO-induced ferroptosis derived from the mouse embryonic fibroblasts cell lines with tamoxifen-induced GPX4 KO (Pfa1 line). This model (Pfa1 immortalized cell line) had previously been established and is widely used for ferroptosis investigations [14]. We measured the proteome landscape dynamic for three chemical ferroptosis inducers: erastin, ML210, and L-Buthionine-sulfoximine (BSO). For each drug, we conducted an individual series of liquid chromatography–mass spectrometry (LC-MS/MS)-based shotgun proteomics in three time points: control 0 h, 24 h, and 48 h after the treatment. Four biological replicates in two or three technical replicates for each condition in each time point were made in DDA mode (Table 1). In total, 27 samples were studied in the ML210 experiment; 24 samples were studied in the erastin experiment; and 24 samples were studied in the BSO experiment.

Table 1. List of the LC-MS/MS proteome sequenced samples. The table presents the number of biological samples multiplied (\times) by technical replicates in each of the conditions (ML210, erastin, and BSO) across time points that were sequenced.

Time Points/Condition	Control (0 h)	after 24 h	after 48 h
Erastin	4 \times 2	4 \times 2	4 \times 2
ML210	4 \times 2	1 \times 3, 3 \times 2	2 \times 3, 2 \times 2
BSO	4 \times 2	4 \times 2	4 \times 2

For all samples, we provide both raw and processed data using a publicly available protein exchange repository (PRIDE) with the following unique identifiers: samples from ML210 experiment are available as PXD041327; Erastin—PXD041463; BSO—PXD041415. Raw LC-MS/MS spectra are provided as original Thermo™ RAW format files supplemented by PEAKs files in mzML and mzid formats. For label-free quantification (LFQ) of proteins, we used IonQuant 1.8 after both MSFragger 3.5 spectra alignment and merging technical replicates in the post-search analysis (see methods for details). Thus, we deposited one quantity table per treatment at the protein level for each of the biological replicates in the public repository, PRIDE. These tables are available in the PRIDE repository as combined_protein.tsv and combined_peptide.tsv files. The widely used MaxLFQ metric for the LFQ experiment is shown in these tables in “MaxLFQ Intensity” columns.

Initial quality control analysis revealed high-quality samples with stable protein expression distribution across all samples in each of the experiments (Figure 1) with the median value for log₂-intensities equal to 29.5 (27.5–31.5) across all samples. The total ion chromatograms (TIC) for all experiments are shown in Figure S1.

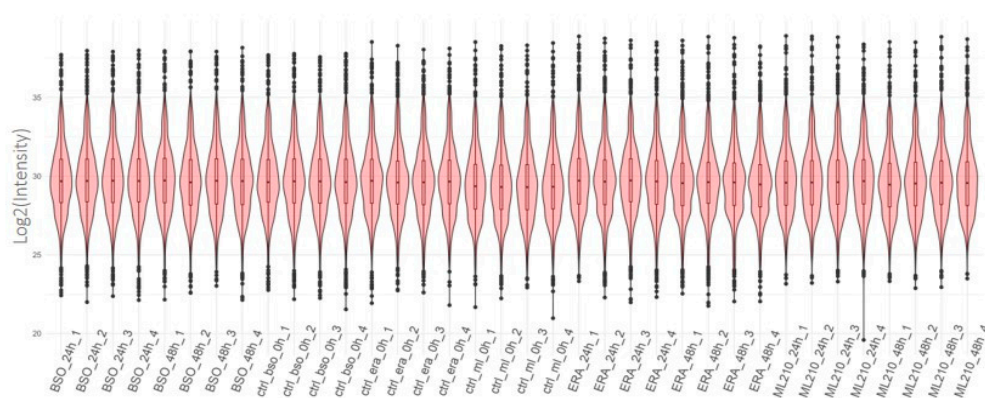


Figure 1. Distribution of the log₂(Intensity) across all detected proteins in each of the samples (x-axis). Number corresponds to the biological replicates. Ctrl—control; ml—ML210; ERA—erastin.

Initially, we detected 3409 proteins in the ML210 experiment, 3942 proteins in the erastin experiment, and 3088 proteins in the BSO experiment. Removing low-confidence proteins (see methods) revealed 2828 proteins in the ML210 experiment, 3061 proteins in the erastin experiment, and 2550 proteins in the BSO experiment, with a similar distribution of non-NA proteins across samples (Figure 2a–c). The sets of proteins detected in different experiments showed a significant overlap; most proteins (2278) were detected in all three experiments (Figure 2d).

In summary, we provide high-quality shotgun proteome data that were obtained during ferroptosis induction by three widely used chemical agents: erastin, ML210, and BSO. All data are publicly available on PRIDE under the following IDs—PXD041463 for erastin, PXD041327 for ML210, and PXD041415 for BSO—both processed and raw files are included. The presence of processed data could provide new information at the protein level and be a valuable source for searching new proteins in ferroptosis-related pathogenesis (e.g., neurodegenerative diseases) or searching for new biomarkers in therapy-resistant cancers. The presence of raw data with the control samples in each of the experiments enables further accurate comparison between these data and newly generated information using similar techniques.

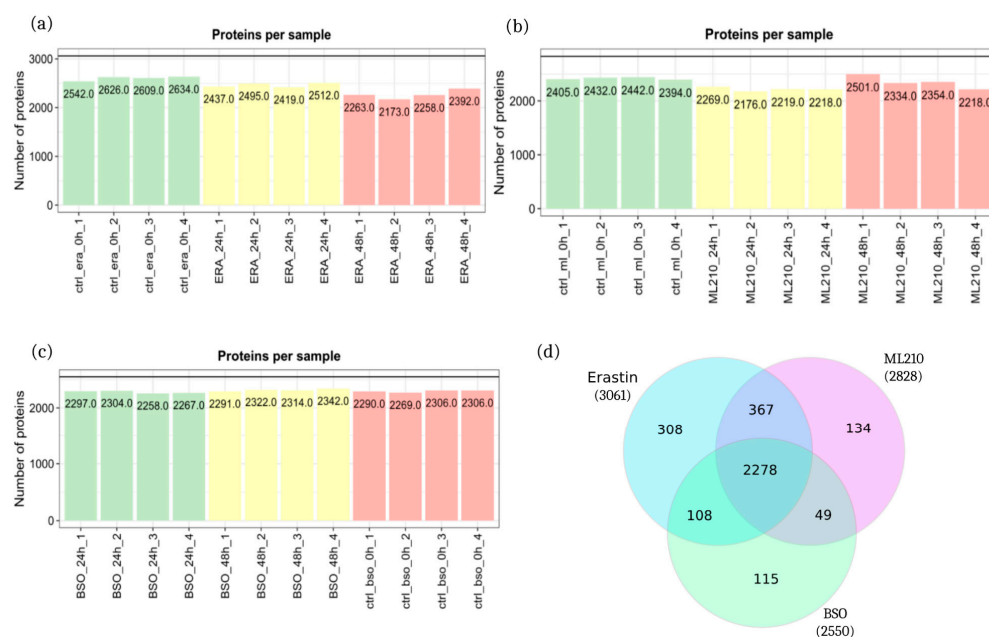


Figure 2. Proteome data overview. (a) Number of detected proteins across biological replicates in the erastin experiment. (b) Number of detected proteins across biological replicates in the ML210 experiment. (c) Number of detected proteins across biological replicates in the BSO experiment. (d) Overlapping of the detected proteins across experiments. ctrl—control; ml—ML210; ERA—erastin. Numbers correspond to the biological replicates.

3. Methods

3.1. Cell Culture

Pfa1 cells, 4-OH-TAM-inducible Gpx4^{-/-} mouse immortalized fibroblasts, were provided by Marcus Conrad (Munich, Germany). Pfa1 cells were cultured in RPMI-1640 medium (PanEko, Moscow, Russia) containing glucose (2 g/L), 10% fetal bovine serum (BioSera, Cholet, France), 2 mM GlutaMAX Supplement (Gibco, Thermo Fisher Scientific, Waltham, MA, USA), and pen/strep (1%) at 37 °C with 5% CO₂ in a humidified incubator (NuAire, Plymouth, MN, USA). For ferroptosis induction, Pfa1 cells (300,000) were seeded on 100 mm tissue-culture-treated culture dishes (#CLS430167, Corning, Corning, NY, USA) and incubated overnight. The next day, cells were treated with or without: (i) 0.3 μM ML210 (SML0521, Sigma-Aldrich, Burlington, MO, USA); (ii) 0.5 μM erastin (E7781, Sigma-Aldrich); (iii) 50 μM L-Buthionine-sulfoximine (B2515, Sigma-Aldrich). Cells were collected for further analysis 24 h and 48 h after treatment.

3.2. Protein Extraction and Preparation for MS Analysis

The original trifluoroethanol (TFE)-based protocol [15] was modified for sample preparation. Cells (approximately 1 million) were washed (×3) with PBS, then treated with 80% cold methanol, scraped out, incubated (1 h, −80 °C), and centrifuged. The pellets were washed with cold acetone, centrifuged, and dried in air. The proteins were redissolved by ultrasonication in 120 μl of 50 mM ammonium-bicarbonate (ABC) buffer, pH 8.0, mixed with TFE (1:1), then +5 mM TCEP (1 h, 50 °C) and +15 mM iodoacetamide (1 h, RT). The samples were diluted 4 times with ABC buffer, 2 μg of trypsin/LysC mix was added, the mixture was incubated (overnight, 37 °C), and the reaction was stopped by adding formic acid (1%). Peptides were dried in a vacuum centrifuge (45 °C, 3 h), redissolved, and measured with a BCA assay.

3.3. LC-MS/MS Analyses

LC-MS/MS was performed on a Q Exactive HF-X mass-spectrometer (Thermo Scientific, Dreieich, Germany) coupled with UltiMate 3000 nano-flow liquid chromatography

system (Thermo Scientific, Dreieck, Germany). Here, 1 µg of peptide mixture was loaded onto an Acclaim µ-Precolumn enrichment column (Thermo Scientific, Vilnius, Lithuania, 0.5 mm × 3 mm, 5 µm) at 5 µL/min flow for 5 min in isocratic mode using buffer C as the mobile phase (2% Acetonitrile, 0.1% formic acid in DI water). Then, the peptides were separated on an Acclaim Pepmap C18 column (75 µm × 500 mm, 3 µm) (in the ERA and ML210 experiments) or an Acclaim Pepmap RSLC column (75 µm × 750 mm, 1.7 µm) (in the BSO experiment) in a gradient of solvents A and B, where A is 0.1% formic acid, B is 80% acetonitrile, and 0.1% formic acid in DI water, at a flow rate 0.3 µL/min. In the ERA and ML210 experiments, the gradient consisted of the following steps: 4% B (5 min), 4 to 33% B (100 min), 33 to 45% B (30 min), 45 to 95% B (1 min), 95% B (20 min), 95 to 4% B (1 min), and 4% B (30 min), while in the BSO experiment the steps were: 4% B (6 min), 4 to 30% B (95 min), 30 to 50% B (25 min), 50 to 95% B (2 min), 95% B (15 min), 95 to 4% B (2 min), and 4% B (20 min).

MS/MS analysis was performed in positive ionization mode using a NanoFlex source. The parameters for the MS/MS analysis were as follows: emitter voltage, 2.2 kV; capillary temperature, 260 °C. Panoramic scan: mass range, 350–1500 *m/z*; resolution, 60,000. Tandem scan: mass range, 100 *m/z*; precursor *m/z*, resolution 15,000. Isolation window: ±0.6 Da. DDA mode was set to “top20”, the intensity cutoff limit for precursor selection was 44,000; NCE: 28 units. Only ions with charge states from +1 to +6 were sent to tandem scanning. The maximum accumulation time was 60 ms for precursor ions and 45 ms for fragment ions. The AGC values for precursor ions were 3×10^6 , and 2×10^5 for fragment ions. All the measured precursor ions were dynamically excluded from the tandem MS/MS analysis for 30 s.

Four biological replicates were prepared, and two technical replicates were acquired for each sample: all these LC-MS2 spectra have been uploaded.

3.4. Data Processing and Protein Identification

Raw files were converted into *.mzML format using the msConvert console application [16]. TIC was built with the xcms R library from MS1 spectra [17]. The Savitzky–Golay algorithm was used for slight peak smoothing (with a parameter of half a window size = 5) [18]. Next, we used MSFragger 3.5 to align spectra to the protein reference with the following parameters: true precursor tolerance, 12 ppm; fragment mass tolerance, 50 mDa [19]. As a reference we used the standard mouse SwissProt proteome (UP000000589) augmented with standard contaminants of the Philosopher package [20] with FBS contaminants previously measured in our lab on FBS samples with the same instrument. To exclude false-positive results, we performed target-decoy analysis on the samples with grouped technical replicates using peptideProphet [21], employing proteinProphet [22] for further statistical clarification. Label-free quantification was conducted by IonQuant 1.8 [23] with the match-between-run option turned on. Next, low covered proteins were filtered out if they were covered by fewer than two unique/razor peptides. The DEP package [24] was used for visualization of the protein numbers. We applied the described data processing protocol in our previously study [25].

Supplementary Materials: The following supporting information can be downloaded at: <https://www.mdpi.com/article/10.3390/data8070119/s1>, Figure S1: Total ion chromatogram (TIC).

Author Contributions: Conceptualization, A.G.S., A.M.N., and O.M.K.; validation, O.M.K. and A.M.N.; formal analysis, O.M.K. and A.M.N.; investigation, D.A.K. and V.K.S.; resources, A.G.S.; data curation, O.M.K. and A.M.N.; writing—original draft preparation, O.M.K., V.K.S., and V.M.T.; writing—review and editing, A.G.S., O.M.K., and A.M.N.; visualization, O.M.K.; supervision, V.V.B.; project administration, A.G.S.; funding acquisition, A.G.S. All authors have read and agreed to the published version of the manuscript.

Funding: This research was funded by the Russian Science Foundation (RSF), grant number 21-74-00140.

Institutional Review Board Statement: Not applicable, all experiments were performed on immortalized cell line.

Informed Consent Statement: Not applicable.

Data Availability Statement: The mass spectrometry proteomics data have been deposited to the ProteomeXchange Consortium via the PRIDE [26] partner repository with the following dataset identifiers: erastin experiment—PXD041463; ML210 experiment—PXD041327; BSO—PXD041415.

Acknowledgments: We thank Marcus Conrad for providing the Pfa1 cell line. This work was partially performed using the equipment of Center for Precision Genome Editing and Genetic Technologies for Biomedicine, Pirogov Russian National Research Medical University, Moscow, Russia.

Conflicts of Interest: The authors declare no conflict of interest.

References

1. Jiang, X.; Stockwell, B.R.; Conrad, M. Ferroptosis: Mechanisms, Biology and Role in Disease. *Nat. Rev. Mol. Cell Biol.* **2021**, *22*, 266–282. [[CrossRef](#)]
2. Gao, M.; Monian, P.; Pan, Q.; Zhang, W.; Xiang, J.; Jiang, X. Ferroptosis Is an Autophagic Cell Death Process. *Cell Res.* **2016**, *26*, 1021–1032. [[CrossRef](#)]
3. Friedmann Angeli, J.P.; Schneider, M.; Proneth, B.; Tyurina, Y.Y.; Tyurin, V.A.; Hammond, V.J.; Herbach, N.; Aichler, M.; Walch, A.; Eggenhofer, E.; et al. Inactivation of the Ferroptosis Regulator Gpx4 Triggers Acute Renal Failure in Mice. *Nat. Cell Biol.* **2014**, *16*, 1180–1191. [[CrossRef](#)]
4. Zheng, J.; Conrad, M. The Metabolic Underpinnings of Ferroptosis. *Cell Metab.* **2020**, *32*, 920–937. [[CrossRef](#)] [[PubMed](#)]
5. Dolma, S.; Lessnick, S.L.; Hahn, W.C.; Stockwell, B.R. Identification of Genotype-Selective Antitumor Agents Using Synthetic Lethal Chemical Screening in Engineered Human Tumor Cells. *Cancer Cell* **2003**, *3*, 285–296. [[CrossRef](#)]
6. Dixon, S.J.; Lemberg, K.M.; Lamprecht, M.R.; Skouta, R.; Zaitsev, E.M.; Gleason, C.E.; Patel, D.N.; Bauer, A.J.; Cantley, A.M.; Yang, W.S.; et al. Ferroptosis: An Iron-Dependent Form of Nonapoptotic Cell Death. *Cell* **2012**, *149*, 1060–1072. [[CrossRef](#)]
7. Eaton, J.K.; Furst, L.; Ruberto, R.A.; Moosmayer, D.; Hilpmann, A.; Ryan, M.J.; Zimmermann, K.; Cai, L.L.; Niehues, M.; Badock, V.; et al. Selective Covalent Targeting of GPX4 Using Masked Nitrile-Oxide Electrophiles. *Nat. Chem. Biol.* **2020**, *16*, 497–506. [[CrossRef](#)] [[PubMed](#)]
8. Reichert, C.O.; de Freitas, F.A.; Sampaio-Silva, J.; Rokita-Rosa, L.; Barros, P.d.L.; Levy, D.; Bydlowski, S.P. Ferroptosis Mechanisms Involved in Neurodegenerative Diseases. *Int. J. Mol. Sci.* **2020**, *21*, 8765. [[CrossRef](#)]
9. Ren, J.-X.; Sun, X.; Yan, X.-L.; Guo, Z.-N.; Yang, Y. Ferroptosis in Neurological Diseases. *Front. Cell. Neurosci.* **2020**, *14*, 218. [[CrossRef](#)]
10. Zhang, C.; Liu, X.; Jin, S.; Chen, Y.; Guo, R. Ferroptosis in Cancer Therapy: A Novel Approach to Reversing Drug Resistance. *Mol. Cancer* **2022**, *21*, 47. [[CrossRef](#)] [[PubMed](#)]
11. Nie, Q.; Hu, Y.; Yu, X.; Li, X.; Fang, X. Induction and Application of Ferroptosis in Cancer Therapy. *Cancer Cell Int.* **2022**, *22*, 12. [[CrossRef](#)]
12. Mishima, E.; Ito, J.; Wu, Z.; Nakamura, T.; Wahida, A.; Doll, S.; Tonnus, W.; Nepachalovich, P.; Eggenhofer, E.; Aldrovandi, M.; et al. A Non-Canonical Vitamin K Cycle Is a Potent Ferroptosis Suppressor. *Nature* **2022**, *608*, 778–783. [[CrossRef](#)] [[PubMed](#)]
13. Zou, Y.; Henry, W.S.; Ricq, E.L.; Graham, E.T.; Phadnis, V.V.; Maretich, P.; Paradkar, S.; Boehnke, N.; Deik, A.A.; Reinhardt, F.; et al. Plasticity of Ether Lipids Promotes Ferroptosis Susceptibility and Evasion. *Nature* **2020**, *585*, 603–608. [[CrossRef](#)]
14. Seiler, A.; Schneider, M.; Förster, H.; Roth, S.; Wirth, E.K.; Culmsee, C.; Plesnila, N.; Kremmer, E.; Rådmark, O.; Wurst, W.; et al. Glutathione Peroxidase 4 Senses and Translates Oxidative Stress into 12/15-Lipoxygenase Dependent- and AIF-Mediated Cell Death. *Cell Metab.* **2008**, *8*, 237–248. [[CrossRef](#)] [[PubMed](#)]
15. Wang, H.; Qian, W.-J.; Mottaz, H.M.; Clauss, T.R.W.; Anderson, D.J.; Moore, R.J.; Camp, D.G.; Khan, A.H.; Sforza, D.M.; Pallavicini, M.; et al. Development and Evaluation of a Micro- and Nanoscale Proteomic Sample Preparation Method. *J. Proteome Res.* **2005**, *4*, 2397–2403. [[CrossRef](#)]
16. Hulstaert, N.; Shofstahl, J.; Sachsenberg, T.; Walzer, M.; Barsnes, H.; Martens, L.; Perez-Riverol, Y. ThermoRawFileParser: Modular, Scalable, and Cross-Platform RAW File Conversion. *J. Proteome Res.* **2020**, *19*, 537–542. [[CrossRef](#)] [[PubMed](#)]
17. Smith, C.A.; Want, E.J.; O’Maille, G.; Abagyan, R.; Siuzdak, G. XCMS: Processing mass spectrometry data for metabolite profiling using nonlinear peak alignment, matching and identification. *Anal. Chem.* **2006**, *78*, 779–787. [[CrossRef](#)]
18. Savitzky, A.; Golay, M.J. Smoothing and differentiation of data by simplified least squares procedures. *Anal. Chem.* **1964**, *36*, 1627–1639. [[CrossRef](#)]
19. Kong, A.T.; Leprevost, F.V.; Avtonomov, D.M.; Mellacheruvu, D.; Nesvizhskii, A.I. MSFragger: Ultrafast and Comprehensive Peptide Identification in Mass Spectrometry-Based Proteomics. *Nat. Methods* **2017**, *14*, 513–520. [[CrossRef](#)]
20. da Veiga Leprevost, F.; Haynes, S.E.; Avtonomov, D.M.; Chang, H.-Y.; Shanmugam, A.K.; Mellacheruvu, D.; Kong, A.T.; Nesvizhskii, A.I. Philosopher: A Versatile Toolkit for Shotgun Proteomics Data Analysis. *Nat. Methods* **2020**, *17*, 869–870. [[CrossRef](#)]
21. Keller, A.; Nesvizhskii, A.I.; Kolker, E.; Aebersold, R. Empirical Statistical Model To Estimate the Accuracy of Peptide Identifications Made by MS/MS and Database Search. *Anal. Chem.* **2002**, *74*, 5383–5392. [[CrossRef](#)] [[PubMed](#)]

22. Nesvizhskii, A.I.; Keller, A.; Kolker, E.; Aebersold, R. A Statistical Model for Identifying Proteins by Tandem Mass Spectrometry. *Anal. Chem.* **2003**, *75*, 4646–4658. [[CrossRef](#)]
23. Yu, F.; Haynes, S.E.; Nesvizhskii, A.I. IonQuant Enables Accurate and Sensitive Label-Free Quantification With FDR-Controlled Match-Between-Runs. *Mol. Cell. Proteomics* **2021**, *20*, 100077. [[CrossRef](#)] [[PubMed](#)]
24. Zhang, X.; Smits, A.; van Tilburg, G.; Ovaa, H.; Huber, W.; Vermeulen, M. Proteome-wide identification of ubiquitin interactions using UblA-MS. *Nat. Protocols* **2018**, *13*, 530–550. [[CrossRef](#)]
25. Nesterenko, A.M.; Korzhenevskii, D.A.; Tereshchuk, V.M.; Kudryashova, O.M.; Belousov, V.V.; Shokhina, A.G. Dataset on the proteomic response during ferroptosis induction via tamoxifen induced GPX4 KO in mouse embryonic fibroblasts. *Data Brief* **2023**, *48*, 109170. [[CrossRef](#)] [[PubMed](#)]
26. Perez-Riverol, Y.; Bai, J.; Bandla, C.; García-Seisdedos, D.; Hewapathirana, S.; Kamatchinathan, S.; Kundu, D.J.; Prakash, A.; Frericks-Zipper, A.; Eisenacher, M.; et al. The PRIDE Database Resources in 2022: A Hub for Mass Spectrometry-Based Proteomics Evidences. *Nucleic Acids Res.* **2022**, *50*, D543–D552. [[CrossRef](#)]

Disclaimer/Publisher’s Note: The statements, opinions and data contained in all publications are solely those of the individual author(s) and contributor(s) and not of MDPI and/or the editor(s). MDPI and/or the editor(s) disclaim responsibility for any injury to people or property resulting from any ideas, methods, instructions or products referred to in the content.